

Stereoselectivity Inversion: Isospecific Propylene Polymerization Catalyzed by Rigid Cyclic Bis(phenoxyaldimine) Titanium Complexes

Xiangxiang Zhao, Zhongtao Chen, Hao Li, and Yuguo Ma*

Cite This: *Macromolecules* 2020, 53, 3806–3813

Read Online

ACCESS |

Metrics & More

Article Recommendations

Supporting Information

ABSTRACT: Precise control over olefin polymerization, especially polymer stereochemistry, through artful catalyst design is attractive and highly challenging. A rigid cyclic framework was first introduced into bis(phenoxyaldimine) titanium catalysts to study its effects on polymerization behaviors. For copolymerization of ethylene with α -olefins and dienes, an improvement in comonomer incorporation ratios was observed while the stereoselectivity and regioselectivity of comonomers were also markedly affected through a unique steric effect. Exceptional regio- and isoselective polymerization of propylene was promoted by the cyclic titanium catalyst via predominately 1,2-insertions and an enantiomeric site control mechanism, contrary to the syndiospecific polymerization by its acyclic analogues. The experimental results revealed that site isomerization was effectively suppressed by ligand cyclization, and inversions of both regio- and stereoselectivity for propylene polymerization were achieved.



INTRODUCTION

Polyolefins materials with excellent properties constitute various kinds of products in everyday life and play an indispensable role in a wide range of fields.¹ Remarkable advances have been made in the development of olefin polymerization catalysts to satisfy the ultimate goal of synthesizing well-defined (co)polymers with controlled molecular weight, molecular weight distribution, sequences, and stereochemistry.^{2–6} Homogeneous catalyst systems, especially non-metallocene catalysts, enable better control over polymer microstructure through devising or adjusting the steric and electronic nature of the ancillary ligands.^{7–16} The bis(phenoxyaldimine) group IV metal complexes are one of the outstanding examples which have been reported by Fujita et al.^{17–21} and Coates et al.^{22–27} Such class of the catalysts centered with titanium metal (Chart 1, I) could promote highly syndiospecific polymerization of propylene in a living manner despite possessing a C_2 -symmetric conformation. The syndiospecific polypropylene is produced via 2,1-insertions of monomer and a chain-end control mechanism.^{20,25,28} The fast fluxional isomerization process of ligands occurring before monomer insertion is responsible for the syndiospecificity.^{29,30}

If the ligand isomerization process is efficiently suppressed, the stereoselectivity of polymerization would change remarkably, and it is promising to obtain isotactic polypropylene by the C_2 -symmetric catalyst. Some attempts on ligand modifications have been reported. Using bis(phenoxyaldimine) zirconium or hafnium complexes, Fujita et al.^{31–33} obtained isotactic polypropylene when $i\text{Bu}_3\text{Al}/[\text{Ph}_3\text{C}][\text{B}(\text{C}_6\text{F}_5)_4]$ was employed as the activator instead of methylaluminoxane (MAO). The ligand was reduced by $i\text{Bu}_3\text{Al}$ in situ to generate

a new sterically bulky phenoxyamido complex (Chart 1, II), which was identified as the actual active species. Coates et al.^{26,27} reported a series of bis(phenoxyketimine) titanium complexes with a phenyl or a bulky alkyl group substituted at the carbon position of the imine moiety (Chart 1, III), which promoted isoselective living propylene polymerization with impeded ligand isomerization. However, some bis(phenoxyaldimine) zirconium complexes^{34,35} designed to bear cyclohexyl or binaphthyl-bridged ligands (Chart 1, IV) yielded atactic polypropylene because of a too open steric environment. Thus, it is still challenging to design well-defined catalysts for control of polymerization stereochemistry.

To provide an alternatively efficient strategy, we herein designed a kind of new bis(phenoxyaldimine) titanium complexes based on rigid cyclic frameworks. A ligand cyclization strategy is proved to be efficient to enhance catalytic behaviors, such as higher thermal stability^{36,37} and polar comonomer incorporation.^{38,39} Our group previously reported a macrocyclic trinuclear nickel complex,⁴⁰ which generated regioregular and highly isotactic polypropylene due to the unique steric effect of the macrocyclic ligand. However, ligand cyclization, usually applied to four-coordinate complexes, had not been introduced into the bis(phenoxyaldimine)

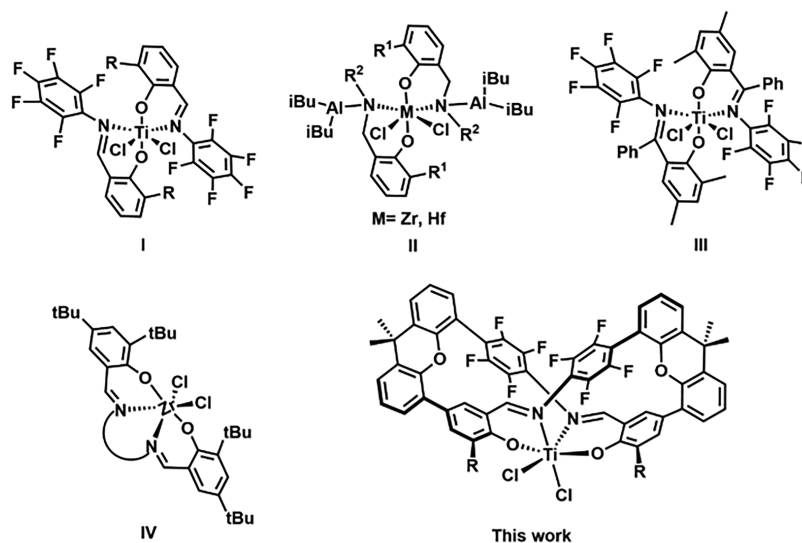
Received: February 28, 2020

Revised: April 28, 2020

Published: May 8, 2020



Chart 1. Selected Examples of Bis(phenoxyimine) Group IV Catalysts for Propylene Polymerization



titanium complexes on account of difficulties of the cyclic ligand design for such octahedral complexes. After careful design of the cyclic ligand, we demonstrated in this work that introducing the rigid cyclic framework could effectively inhibit the ligand isomerization process and change the regio- and stereoselectivity of propylene polymerization.

EXPERIMENTAL SECTION

General Considerations. All manipulations of air- and/or water-sensitive compounds were carried out under a dry nitrogen atmosphere using standard Schlenk techniques or in a nitrogen-filled mBraun glovebox with a high-capacity recirculator (<5 ppm of O₂/H₂O). All solvents for high-vacuum line manipulations were purified by passing through the mBraun solvent purification system and stored under nitrogen over activated 4 Å molecular sieves in resealable flasks. Commercial ethylene and propylene were used directly for polymerization without further purification. 1-Hexene and other monomers for polymerization were distilled from CaH₂ prior to use. Methylaluminoxane (MAO, 10 wt % Al in toluene) provided by Sinopec Yanshan Petrochemical Company was used without further treatment. All of the other reagents were purchased and used as received.

¹H and ¹³C NMR spectra were recorded on Bruker-400 (400 MHz) and Bruker-500 (500 MHz) spectrometers using CDCl₃ as solvent. Chemical shifts are reported in parts per million (ppm), and coupling constants are reported in hertz (Hz). ¹H NMR chemical shifts were referenced versus internal tetramethylsilane (0 ppm); ¹³C NMR chemical shifts were referenced versus chloroform-*d* (77.16 ppm) or 1,1,2,2-tetrachloroethane-*d*₂ (73.78 ppm). ¹⁹F NMR spectra were recorded on a Bruker-500 (500 MHz), and chemical shifts are referenced to CF₃COOH as an external standard. Quantitative ¹³C NMR analysis of polymers was performed at 90 °C using an inverse gated decoupling sequence with a 2.0 s acquisition time and 10 s delay time. Mass spectra were recorded on a VG ZAB-HS mass spectrometer. Single-crystal X-ray diffraction data were collected with a NONIUS Kappa CCD diffractometer with a graphite monochromator and Mo Kα radiation [$\lambda(\text{Mo K}\alpha) = 0.71073 \text{ \AA}$]. Structures were solved by direct methods with SHELXS-97 and refined against *F*² with SHELXS-97. Polymer melting points were measured by differential scanning calorimetry (DSC) using a TA DSC Q100 instrument, and data were collected from the second heating run at a heating rate of 10 °C/min. High-temperature gel permeation chromatography (GPC) was performed on an Agilent PL-GPC 220 equipped with a refractive index (RI) detector. The GPC column set (two PLgel mixed-B, 7.5 mm × 300 mm, 10 μm) was eluted with

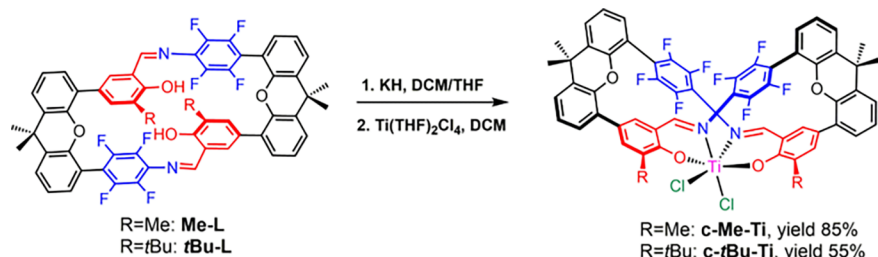
1,2,4-trichlorobenzene (TCB) at 150 °C with a rate of 1.0 mL/min. GPC data calibration was done with unimodal polystyrene standards and corrected by universal calibration using the Mark–Houwink parameters: $K = 4.06 \times 10^{-2} \text{ cm}^3/\text{g}$, $\alpha = 0.727$ and $K = 1.56 \times 10^{-2} \text{ cm}^3/\text{g}$, $\alpha = 0.67$ for polyethylene and polypropylene, respectively.

General Procedure for Ethylene Polymerization. Ethylene polymerizations were carried out in 250 mL three-neck flasks equipped with a large magnetic stirring bar. For this experiment, a preassembled, degassed reactor containing toluene (50 mL) and MAO was presaturated under ethylene (1 atm) and equilibrated at the desired temperature using an external bath. The required amount of titanium complex was dissolved in toluene (2 mL) at room temperature, and the solution was added to the reactor via a gastight syringe to initiate the polymerization. After a given period of time, polymerization was quenched by addition of acidified ethanol (2 mL). The polymer was precipitated in acidified methanol (2% v/v, 300 mL), collected by filtration, washed with methanol, and dried in a vacuum at 80 °C overnight until achieving a constant weight.

General Procedure for Propylene Polymerization. In the glovebox, a 350 mL heavy-walled glass reactor (dried in an oven at 120 °C overnight before use) equipped with a stirring bar was loaded with toluene (50 mL) and MAO. The reactor was then taken out and interfaced to the propylene gas. The solution was saturated with propylene (50 psi) at the desired temperature for 30 min. A toluene solution (3 mL) of precatalyst was injected via a gastight syringe to initiate the polymerization. After the desired time, the reactor was quenched with methanol and vented. The polymer was precipitated in a mixed solution of HCl/methanol (2% v/v, 500 mL), collected by filtration, washed with methanol, and dried in a vacuum at 60 °C overnight until achieving a constant weight.

General Procedure for Copolymerization of Ethylene and Comonomer. Copolymerizations were carried out in 250 mL three-neck flasks equipped with a large magnetic stirring bar. In a typical experiment, the comonomer was injected into a preassembled, degassed reactor containing toluene (45 mL) and MAO. The solution was presaturated with ethylene at 40 °C using an external bath. The required amount of the titanium catalyst was dissolved in toluene (5 mL) under nitrogen atmosphere. The solution was injected into the reactor to initiate the polymerization. After 1 h, the polymerization was quenched by addition of acidified ethanol (2 mL). The copolymer was precipitated in acidified methanol (2% v/v, 300 mL), collected by filtration, washed with methanol, and dried in a vacuum at 80 °C overnight until achieving a constant weight.

Scheme 1. Synthesis of the Cyclic Titanium Complexes



RESULTS AND DISCUSSION

Synthesis and Characterization of Ligands and Complexes.

The preligands were prepared by successive two-step Suzuki couplings of the xanthene skeleton with the corresponding aniline or salicylaldehyde. Intermolecular self-condensation of the preligands afforded the well-designed cyclic ligands (Scheme S1). Through X-ray single-crystal diffraction analysis, the cyclic ligands possessed a C_2 -symmetric double-decker conformation (Figures S49 and S50 in the Supporting Information). The distances between the coordinated atoms (O–O, N–N) in the cyclic ligands were all short (<3.3 Å) enough for successful metalation subsequently. The cyclic bis(phenoxyaldimine) titanium complexes with different substituents at the ortho position of the phenolate rings were successfully prepared with moderate yields under a mild metalation procedure (Scheme 1).⁴¹ The C_2 -symmetric structures of these complexes were well maintained in solution as suggested by ¹H and ¹⁹F NMR spectra (see Figures S17–S22). As for **c-Me-Ti**, no conformation isomer was observed in CDCl₃ solution even at low temperature (233 K) by ¹H NMR and ¹⁹F NMR spectra (see Figure S23). In contrast, **c-tBu-Ti** possessed more than one conformation isomer probably due to restricted conformation rotation with the bulky tBu groups (see Figures S22 and S24).

The single-crystal structure of **c-Me-Ti** revealed a C_2 -symmetric and distorted octahedral geometry conformation with a *trans*-O, *cis*-N, and *cis*-Cl disposition (Figure 1). The bond lengths of Ti–N, Ti–O, and Ti–Cl are similar to those of typical bis(phenoxyaldimine) titanium complexes reported previously (comparison data collected in Table S6 of the Supporting Information), suggesting a similar electronic environment at the titanium center. By comparison, **c-Me-Ti** possesses distinctly narrower N–Ti–N angles, torsion angles (Ti–N–C–C), and dihedral angles involving the aniline moiety and phenoxy planes, implying a relatively more open steric environment. As observed, the aniline moieties and the phenolate rings are forced to compress toward each other by rigid xanthene linkers, resulting in the skeleton distortion and the narrower angles. Moreover, the spatial distances between the ortho fluorine atoms of the aniline moiety and the chloride atoms bound to the titanium are much shorter (~3 Å). Therefore, the adjacent fluorine atoms could cause a non-negligible change on the steric environment.

To better compare the steric properties of the cyclic catalysts and traditional acyclic catalysts, the topographic steric maps of acyclic catalyst **Me-Ti** and cyclic catalyst **c-Me-Ti** were generated by the SambVca 2.0 program⁴² (Figure 2). Catalyst **c-Me-Ti** had a slightly lower percentage of buried volume in total (%*V*_{Bur}, 61.3 vs 61.9) due to distortion of the skeleton. Note that in catalyst **c-Me-Ti**, locally larger steric hindrance resulting from the ortho F atoms existed in the NW and SE

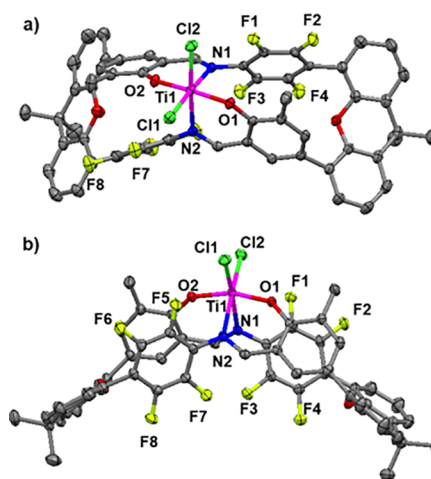


Figure 1. (a) Crystal structure of **c-Me-Ti** with thermal ellipsoids at the 50% probability level. Hydrogens have been omitted for clarity. Selected bond lengths (Angstroms) and bond angles (degrees): Ti–O(1) 1.8410(1), Ti–O(2) 1.8421(1), Ti–Cl(1) 2.2724(4), Ti–Cl(2) 2.2756(4), Ti–N(1) 2.3177(1), Ti–N(2) 2.3139(1); Cl(1)–Ti–Cl(2) 94.32(1), O(1)–Ti–O(2) 161.78(4), N(1)–Ti–N(2) 79.03(4). (b) Top view.

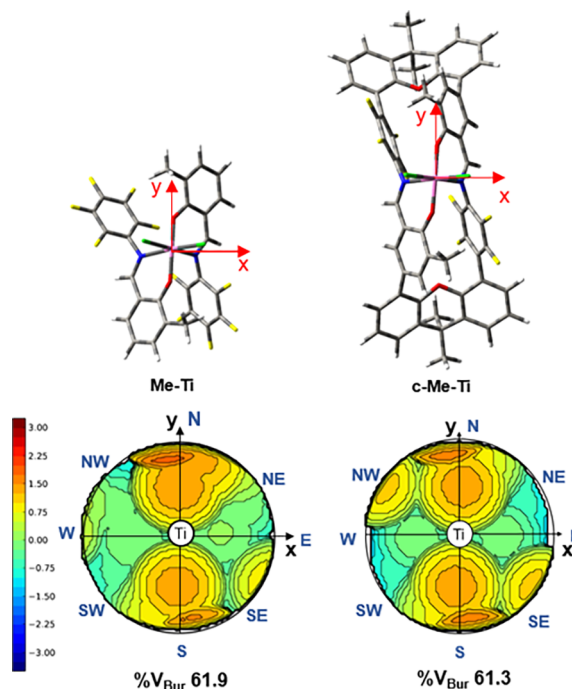


Figure 2. Steric maps of cyclic catalyst **c-Me-Ti** and the corresponding acyclic catalyst **Me-Ti**.

Table 1. Results of Ethylene Polymerization^a

entry	complex	T (°C)	t (min)	yield (g)	TOF ^b	M _w ^c (×10 ⁴)	Đ ^c	T _m ^d (°C)
1	c-Me-Ti	0	5	0.242	5.81	27.0	3.63 ^e	134.4
2	c-Me-Ti	25	5	0.183	4.39	9.86	2.13	134.4
3	c-Me-Ti	40	5	0.521	12.5	6.95	2.18	131.5
4	c-Me-Ti	60	5	0.464	11.1	5.36	1.77	132.3
5	c-Me-Ti	80	5	0.496	11.9	3.26	1.65	127.4
6	c-tBu-Ti	0	1	0.341	102	36.9	2.36	135.8
7	c-tBu-Ti	25	1	0.330	99.0	61.6	2.14	134.9
8	c-tBu-Ti	25	5	0.815	48.8	141	2.28	134.7
9	c-tBu-Ti	40	1	0.398	119	50.9	1.74	135.6
10	c-tBu-Ti	40	5	0.907	54.4	85.8	2.83	134.4
11	c-tBu-Ti	60	1	0.437	131	39.1	2.21	134.3
12	c-tBu-Ti	80	1	0.324	97.2	29.1	2.58	134.4
13 ^f	Me-Ti	40	5	0.438	26.3	47.4	2.00	140.0
14 ^f	tBu-Ti	40	5	0.846	50.8	99.2	2.52	139.0

^aPolymerization conditions: complex c-Me-Ti (5 μmol) or c-tBu-Ti (2 μmol), cocatalyst MAO (Al/Ti = 1000), toluene 50 mL, ethylene pressure 1 atm. ^bIn 10⁵ g polymer (mol Ti)⁻¹ h⁻¹. ^cMolecular weight and dispersity (Đ) were determined by GPC using polystyrene standard. ^dDetermined by DSC from the second melting curve. ^eBimodal distribution. ^fPolymerization data of acyclic catalysts were cited from ref 41. Polymerization conditions: titanium complex (2 μmol), dried MAO (Al/Ti = 250).

Table 2. Results of Copolymerization^a

entry	complex (μmol)	comonomer	yield (g)	TOF ^b	M _w ^c (×10 ⁴)	Đ ^c	T _m ^d (°C)	X (%) ^e	micro: ^f (%)
1	c-Me-Ti (5)	1-hexene	0.089	1.78	17.6	2.92		28.2	
2	Me-Ti ^g (10)	1-hexene	0.215	2.15	16.3	3.23		25.2	
3	c-tBu-Ti (5)	1-hexene	0.078	1.56	6.48	2.51	72.3	10.6	
4	tBu-Ti ^g (5)	1-hexene	0.088	1.76	30.8	5.01	106	4.5	
5	c-Me-Ti (10)	isoprene	0.013	0.13	9.41	10.2	130.3	12.1	78
6	Me-Ti ^g (10)	isoprene	0.016	0.16	2.86	3.55	127.3	5.5	81
7	c-tBu-Ti (5)	isoprene	0.159	3.18	22.0	3.70	133.9	51.0	78
8	tBu-Ti ^g (5)	isoprene	0.085	1.70	4.97	5.39	132.5	51.3	86
9	c-Me-Ti (5)	1,5-HD	0.153	3.06	5.89	3.46	36.8	31.9	79
10	Me-Ti ^g (10)	1,5-HD	0.291	2.91	8.76	2.47	55.7	40.8	93
11	c-tBu-Ti (5)	1,5-HD	0.52	10.4	10.1	3.88	42.1	18.4	29
12	tBu-Ti ^g (5)	1,5-HD	0.106	2.12	21.9	2.78	105.4	6.9	54

^aPolymerization conditions: cocatalyst MAO (Al/Ti = 1000), toluene 50 mL, T = 40 °C, time 1 h, ethylene 1 atm, comonomer concentration 1 M. ^bIn 10⁴ g of polymer (mol Ti)⁻¹ h⁻¹. ^cMolecular weight and dispersity (Đ) were determined by GPC using polystyrene standard. ^dDetermined by DSC from the second melting curve. ^eMolar incorporation ratios of comonomer determined by ¹H NMR or ¹³C NMR spectra. ^fMicrostructure analysis: the ratios of 1,4-IP for isoprene copolymerization and ratios of *trans*-MCP unit in 1,5-HD incorporation, respectively. ^gCatalysts based on acyclic ligands were synthesized according to the literature⁴¹ for better comparison.

quadrants, which further confirmed the speculation mentioned above. Therefore, the unique site environment with relatively open and locally crowded steric effect coexistence in the cyclic catalysts would be expected to have a significant influence on the catalytic behaviors.

Ethylene Homopolymerization. When activated with MAO, the two cyclic catalysts both showed high activity for ethylene polymerization and produced high-molecular-weight polyethylene under different temperatures (Tables 1 and S1). The changes of activities with temperatures followed a similar trend by the two catalysts (Figure S1 in the Supporting Information), in which the activities were relatively higher at 40–60 °C. Cyclic catalyst c-tBu-Ti showed comparable activities (up to 10⁷ g polymer (mol Ti)⁻¹ h⁻¹) with the typical bis(phenoxyaldimine) titanium complex previously reported (Table 1, entry 10 vs 14) and produced high-molecular-weight polyethylene (up to 1.41 × 10⁶ Da). However, as compared with those of acyclic catalyst Me-Ti (Table 1, entry 13), the activity and molecular weight of polyethylene obtained using c-Me-Ti were both relatively lower. Meanwhile, in comparison with c-tBu-Ti, c-Me-Ti

exhibited 2 orders of magnitude lower activity while the molecular weight of polyethylene produced was about 10 times lower due to its less steric hindrance.

Ethylene Copolymerization. The unique steric environment around the metal site in cyclic catalysts encouraged us to further investigate copolymerization behaviors of ethylene with α -olefin, α,ω -dienes, and conjugated dienes. In the copolymerization of ethylene and 1-hexene, higher 1-hexene incorporation ratios were observed by catalysts with a methyl group substituted due to smaller steric hindrance (Table 2, entries 1 and 2). Compared with acyclic catalysts, the two cyclic catalysts both showed higher 1-hexene incorporation ratios (Table 2, entry 1 vs entry 2; entry 3 vs entry 4), suggesting the existence of a more open steric environment in cyclic catalysts. This agreed with the observation from their crystal structures and steric maps *vide supra*. In addition, according to ¹³C NMR spectra (Figures S26 and S28), a few consecutive 1-hexene insertion units existed in the copolymer obtained by cyclic catalyst c-Me-Ti. In contrast, the resonance in the copolymer obtained by acyclic catalyst Me-Ti was not detected.

When isoprene (IP) was used as the comonomer, cyclic catalyst **c-Me-Ti** also exhibited a higher IP incorporation level relative to the acyclic analogue. Although 1,4-enchainments of IP played a dominant role for all catalysts, the ratios of 3,4-insertions were enhanced in the copolymers obtained by cyclic catalysts compared with those by acyclic catalysts (Table 2, entry 5 vs entry 6; entry 7 vs entry 8). This result was probably attributed to the effect of a locally crowded steric environment caused by the near ortho fluorine groups in cyclic catalysts, which also gave rise to the higher molecular weight of copolymers simultaneously.

For copolymerization of ethylene and 1,5-hexadiene (1,5-HD), cyclic catalysts both exhibited higher activities. Catalysts with a methyl group also produced copolymers with a higher amount of 1,5-HD incorporation (Table 2, entries 9 and 10). Incorporation ratios of 1,5-HD comonomer in copolymers could be well adjusted by changing the 1,5-HD concentrations (see Table S2). Also, relatively higher 1,5-HD incorporation ratios were achieved by cyclic catalyst **c-tBu-Ti** (Table 2, entry 11 vs entry 12). Microstructure analysis of copolymers revealed that 1,5-HD monomers incorporated were completely cyclized to methylene-1,3-cyclopentane (MCP) units with no detectable signals associated with cross-links or vinylic end groups. However, the stereochemistry of MCP units in copolymers was quite different in that *trans*-MCP units were mainly formed using catalysts substituted by a methyl group (Table 2, entry 9, **c-Me-Ti**: 79%; entry 10, **Me-Ti**: 93%) while *cis*-MCP units dominated by catalysts with a tBu group (Table 2, entry 11, **c-tBu-Ti**: 29%; entry 12, **tBu-Ti**: 54%). Meanwhile, higher *cis*-MCP contents were obtained by cyclic catalysts relative to acyclic analogues (Table 2, entries 9–12). According to the literature,^{43,44} *trans*-MCP units are usually generated through 1,5-HD monomers adopting the chair-type conformation in the cyclization transition state. When in the presence of more sterically congested catalysts, a twisted boat-type conformation would be accommodated to lead to a *cis* ring (Figure 3).

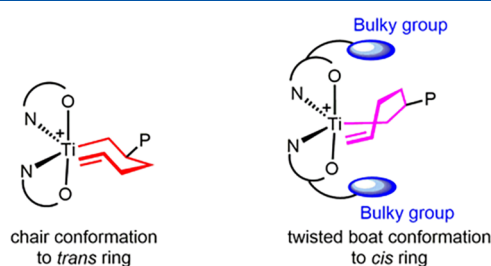


Figure 3. Ring-closure stereochemistry of 1,5-HD in polymerization.

Hence, it is reasonable for the results that with increasing size of the substituents ortho to the phenolate ring, *cis*-MCP ratios in copolymers were improved. As for cyclic catalysts, the more sterically crowded environment from the proximate fluorine could be responsible for the ring-closure stereochemistry observed. It is notable that the predominant insertion stereoselectivity of 1,5-HD changed from *trans* to *cis* fashion by cyclic catalyst **c-tBu-Ti**. From the copolymerization results above, the novel cyclic catalysts with a unique site environment generally exhibited a better capacity of comonomer incorporation and really different regiochemistry and stereochemistry in copolymer structures in comparison with traditional catalysts.

Propylene Polymerization. Next, we focused on the polymerization of propylene by cyclic catalysts to investigate the effect of cyclic ligand on polymerization stereochemistry. The cyclic catalysts were both active for propylene polymerization when activated with MAO (Table 3). It was noteworthy that the activities of propylene polymerization using cyclic catalysts were about 3–4 orders of magnitude lower than those in ethylene polymerization under similar conditions, suggesting that the cyclic catalysts exhibited extremely high monomer selectivity. This was consistent with the results in acyclic bis(phenoxyaldimine) titanium catalysts previously reported.^{19,20} Importantly, in contrast to the acyclic analogous catalysts that generated syndiotactic polypropylene, the polypropylene samples (Table 3, entries 1–4) obtained by **c-Me-Ti** were moderately isotactic ([*mmmm*] up to 59%) with high regioregularity (Figure 4), implying a completely different polymerization mechanism. The ratios of the main pentad signals from stereodeficits (*mmmr* 13%, *mmrr* 12%, and *mmrm* + *rmrr* 8%) was closer to the statistical model of an “enantiomorphic site control” mechanism (*mmmr*:*mmrr*:*mmrm* ≈ 2:2:1), which was well in line with the C_2 -symmetric conformation of the catalyst. Considering that the typical bis(phenoxyaldimine) titanium catalysts promote syndiospecific propylene polymerization via a chain-end control mechanism based on the ligand isomerization process, we demonstrate that in our system the ligand isomerization process was efficiently inhibited by the strategy of ligands cyclization, thus resulting in the isoselectivity via a site control mechanism. In polymerization carried out at higher temperature, the stereoregularity of polypropylenes decreased accompanied by more head-to-head and tail-to-tail misinsertions while isotacticity still remained ([*mm*] > 60%).

To obtain more information on the mechanistic details, chain end analysis was performed using polypropylene with a low molecular weight (Table 2, entry 4). Predominant isobutyl

Table 3. Results of Propylene Polymerization^a

entry	complex	<i>T</i> (°C)	yield (g)	TOF ^b	<i>M_w</i> ^c (×10 ⁴)	<i>D</i> ^c	[<i>mm</i>] ^d (%)	α^e	<i>T_g</i> ^f (°C)	<i>T_m</i> ^f (°C)
1 ^g	c-Me-Ti	−20	0.115	3.83	9.05	5.66 ^j	73	0.89	−15.2	80.9, 141.4
2	c-Me-Ti	0	0.032	1.60	11.8	16.2 ^j	72	0.90	−14.5	142.2
3 ^h	c-Me-Ti	25	0.067	1.34	3.67	4.83	68	0.88	−18.7	72.2, 144.5
4 ⁱ	c-Me-Ti	50	0.010	0.13	2.16	2.11	60			
5 ^k	c-tBu-Ti	−20	0.120	4.80	33.9	7.86	27		−8.7	
6	c-tBu-Ti	0	0.077	3.85	8.07	9.42 ^j	24		−8.3	

^aPolymerization conditions: complex (10 μ mol), cocatalyst MAO (Al/Ti = 1000), toluene (50 mL), propylene pressure (50 psi), time (2 h). ^bIn 10³ g of polymer (mol Ti)^{−1} h^{−1}. ^cDetermined by GPC using polystyrene standard. ^dDetermined by ¹³C NMR spectra. ^eEnantiofacial selectivity parameter, calculated from the equation [*mmmm*] = α^5 + (1 − α)⁵. ^fDetermined by DSC from the second melting curve. ^gTime (3 h). ^hComplex (20 μ mol), time (2.5 h). ⁱComplex (50 μ mol), MAO (400 equiv), time (1.5 h). ^jMultimodal distribution. ^kTime (2.5 h).

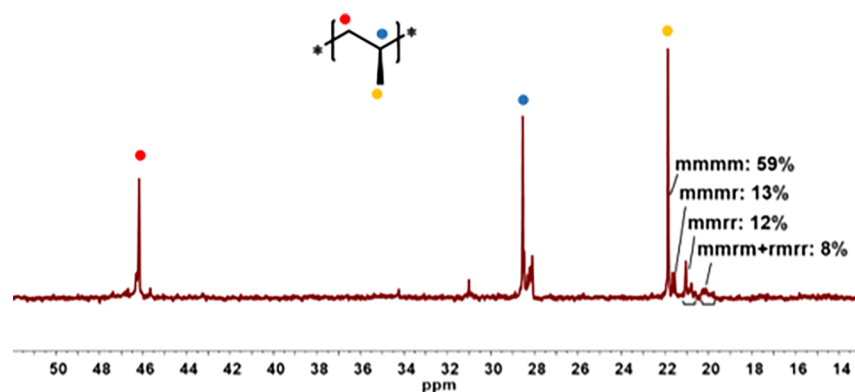


Figure 4. ^{13}C NMR spectrum (125 MHz, $\text{C}_2\text{D}_2\text{Cl}_4$, 90 °C) of polypropylene obtained by *c*-Me-Ti (Table 3, entry 2).

Scheme 2. Proposed Main Insertion Pathways of Propylene Monomer at Initiation, Propagation, and Termination Process for Propylene Polymerization Using Complex *c*-Me-Ti

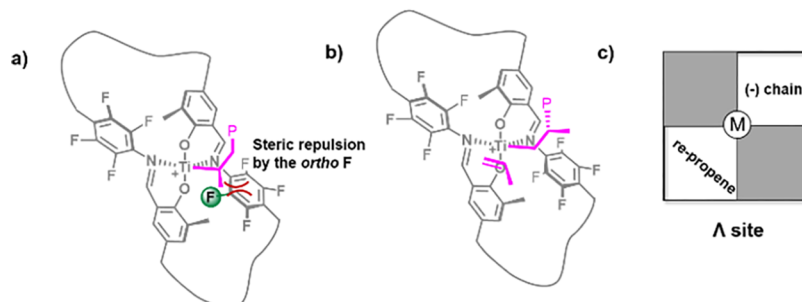
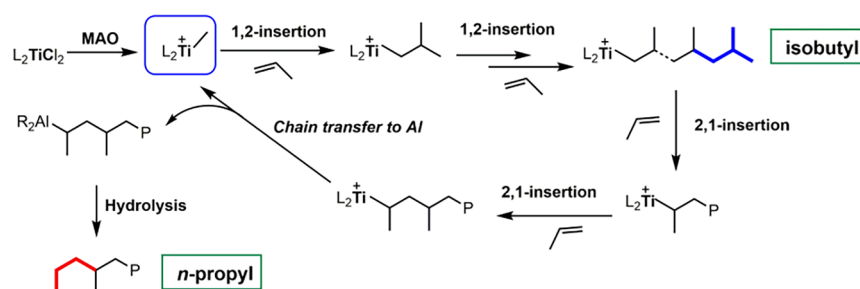


Figure 5. Proposed model for isospecific and 1,2-regiochemistry polymerization of propylene by *c*-Me-Ti. (a) Ti active site with secondary growing chain; (b) transition state for propylene insertion into Ti with primary growing chain; (c) quadrants representation; gray quadrants correspond to relatively crowded zones occupied by fluoroaniline moiety.

(~49%) and *n*-propyl (~51%) end groups were observed and assigned (see Figure S43) according to the literature.^{20,25,45,46} As no unsaturated chain ends resulting from β -hydride/methyl elimination were observed, chain transfer to aluminum would be the main chain release pathway. Therefore, insertion of propylene into Ti–Me species dominated the initiation process. Since other possible ends, especially ethyl, *sec*-butyl, and isopentyl derived from 2,1-insertion of propylene during initiation process, were not explicitly detected, the possibility that propylene underwent 2,1-insertion at an initiation period was disregarded. Combined with the respective contents of the observed chain ends, the isobutyl end groups were mainly regarded as initiation ends, which were derived from exclusively consecutive 1,2-insertions of propylene into the Ti–Me species. Generally speaking, an occasional 2,1-insertion would make the next monomer insertion slow, which promoted chain transfer in the following. Reasonably, the *n*-propyl end groups were formed in the termination steps by chain transfer to aluminum and the following hydrolysis of

titanium-bound secondary growing chain after two consecutive 2,1-insertions. The speculated main insertion pathways of propylene are shown in Scheme 2. Therefore, it could be concluded that in propylene polymerization with cyclic catalyst *c*-Me-Ti, selective 1,2-insertions occurred in the initiation and propagation steps while occasional 2,1-misinsertions would lead to the termination process.

According to the discussions above, in propylene polymerization, the inversions from selective 2,1-insertions and syndiospecificity by acyclic catalysts to 1,2-insertions and isoselectivity by cyclic complex *c*-Me-Ti were achieved. Ligand cyclization makes the catalyst relatively rigid to maintain its C_2 -symmetric conformation. The proposed mechanism model is shown in Figure 5. When the Ti center is bound with a secondary growing chain resulting from 2,1-insertions of propylene, stronger steric repulsion between the methyl of C_α in the chain and the adjacent fluorine groups would disfavor the conformation, which is probably an important reason for the regioselectivity inversion. In the transition state of

insertion, the primary growing chain bound to the Ti center adopts the most favorable orientation to minimize the steric interactions with the ligand (Figure 5b, (–) chain). The incoming monomer prefers *re* enantiofacial coordination, which is in anti fashion relative to the growing chain to avoid steric congestion. The situation is sketched in the quadrants representation shown in Figure 5c. For catalyst **c-Ti**, the polypropylene obtained had stereoirregular microstructure though with higher regioregularity (see Figures S45 and S46). Through analysis of the possible transition state structure, we think the bulky substituents at the ortho position of the phenolate rings would also have steric repulsion with the methyl group of 1,2-oriented propylene and growing chain. The orientation selectivity of monomer and growing chain is disfavored by the overly crowded environment, thus resulting in atactic polypropylene. These results suggested that an appropriate steric environment around the metal center is crucial for polymerization stereochemistry.

CONCLUSIONS

In summary, we reported the synthesis of two new cyclic bis(phenoxyaldimine) titanium catalysts for olefin (co)-polymerization. The unique steric environment endowed the catalysts with improved copolymerization capability and controllable regio- or stereochemistry of comonomer units. More importantly, the polypropylenes produced by **c-Me-Ti** were moderately isotactic with high 1,2-regioselectivity via an “enantiomorphic site control” mechanism, which were totally different from traditional catalysts. In fact, this is a rare example for achieving inversions of both regio- and stereoselectivity in propylene polymerization by such type of bis(phenoxyaldimine) titanium complexes. The results demonstrate that the ligand cyclization is an efficient and alternative strategy for maintaining the conformation stability and regulating polymerization stereochemistry.

ASSOCIATED CONTENT

Supporting Information

The Supporting Information is available free of charge at <https://pubs.acs.org/doi/10.1021/acs.macromol.0c00468>.

Detailed synthesis of ligands and complexes, characterization data, additional polymerization results, crystallographic data, and calculations (PDF)

Crystallographic data for ligand **Me-L** (CIF)

Crystallographic data for ligand **tBu-L** (CIF)

Crystallographic data for complex **c-Me-Ti** (CIF)

AUTHOR INFORMATION

Corresponding Author

Yuguo Ma – Beijing National Laboratory for Molecular Sciences (BNLMS), Center for Soft Matter Science and Engineering, Key Lab of Polymer Chemistry & Physics of Ministry of Education, College of Chemistry, Peking University, Beijing 100871, China; orcid.org/0000-0002-6174-8720; Email: ygma@pku.edu.cn

Authors

Xiangxiang Zhao – Beijing National Laboratory for Molecular Sciences (BNLMS), Center for Soft Matter Science and Engineering, Key Lab of Polymer Chemistry & Physics of Ministry of Education, College of Chemistry, Peking University, Beijing 100871, China

Zhongtao Chen – Beijing National Laboratory for Molecular Sciences (BNLMS), Center for Soft Matter Science and Engineering, Key Lab of Polymer Chemistry & Physics of Ministry of Education, College of Chemistry, Peking University, Beijing 100871, China

Hao Li – Beijing National Laboratory for Molecular Sciences (BNLMS), Center for Soft Matter Science and Engineering, Key Lab of Polymer Chemistry & Physics of Ministry of Education, College of Chemistry, Peking University, Beijing 100871, China

Complete contact information is available at: <https://pubs.acs.org/10.1021/acs.macromol.0c00468>

Notes

The authors declare no competing financial interest.

ACKNOWLEDGMENTS

This work was financially supported by National Natural Science Foundation of China (NSFC, 21871016 and 51573002). Computational work was supported by the High-Performance Computing Platform of Peking University.

REFERENCES

- (1) Kaminsky, W. Trends in Polyolefin Chemistry. *Macromol. Chem. Phys.* **2008**, *209*, 459–466.
- (2) Natta, G.; Pino, P.; Corradini, P.; Danusso, F.; Mantica, E.; Mazzanti, G.; Moraglio, G. Crystalline Polymers of α -Olefins. *J. Am. Chem. Soc.* **1955**, *77*, 1708–1710.
- (3) Alt, H. G.; Köppl, A. Effect of the Nature of Metallocene Complexes of Group IV Metals on Their Performance in Catalytic Ethylene and Propylene Polymerization. *Chem. Rev.* **2000**, *100*, 1205–1222.
- (4) Coates, G. W. Precise Control of Polyolefin Stereochemistry Using Single-Site Metal Catalysts. *Chem. Rev.* **2000**, *100*, 1223–1252.
- (5) Marks, T. J. Surface-bound Metal Hydrocarbyls. Organometallic Connections between Heterogeneous and Homogeneous Catalysis. *Acc. Chem. Res.* **1992**, *25*, 57–65.
- (6) Makio, H.; Terao, H.; Iwashita, A.; Fujita, T. FI Catalysts for Olefin Polymerization—A Comprehensive Treatment. *Chem. Rev.* **2011**, *111*, 2363–2449.
- (7) Gibson, V. C.; Spitzmesser, S. K. Advances in Non-Metallocene Olefin Polymerization Catalysis. *Chem. Rev.* **2003**, *103*, 283–316.
- (8) Ittel, S. D.; Johnson, L. K.; Brookhart, M. Late-Metal Catalysts for Ethylene Homo- and Copolymerization. *Chem. Rev.* **2000**, *100*, 1169–1204.
- (9) Mu, H.; Pan, L.; Song, D.; Li, Y. Neutral Nickel Catalysts for Olefin Homo- and Copolymerization: Relationships between Catalyst Structures and Catalytic Properties. *Chem. Rev.* **2015**, *115*, 12091–12137.
- (10) Johnson, L. K.; Killian, C. M.; Brookhart, M. New Pd(II)- and Ni(II)-Based Catalysts for Polymerization of Ethylene and α -Olefins. *J. Am. Chem. Soc.* **1995**, *117*, 6414–6415.
- (11) Killian, C. M.; Tempel, D. J.; Johnson, L. K.; Brookhart, M. Living Polymerization of α -Olefins Using Ni(II)- α -Diimine Catalysts. Synthesis of New Block Polymers Based on α -Olefins. *J. Am. Chem. Soc.* **1996**, *118*, 11664–11665.
- (12) Guan, Z.; Cotts, P. M.; McCord, E. F.; McLain, S. J. Chain Walking: A New Strategy to Control Polymer Topology. *Science* **1999**, *283*, 2059–2062.
- (13) Younkin, T. R.; Connor, E. F.; Henderson, J. I.; Friedrich, S. K.; Grubbs, R. H.; Bansleben, D. A. Neutral, Single-Component Nickel (II) Polyolefin Catalysts That Tolerate Heteroatoms. *Science* **2000**, *287*, 460–462.
- (14) Wang, F.-Z.; Tian, S.-S.; Li, R.-P.; Li, W.-M.; Chen, C.-L. Ligand Steric Effects on Naphthyl- α -diimine Nickel Catalyzed α -Olefin Polymerization. *Chin. J. Polym. Sci.* **2018**, *36*, 157–162.

- (15) Xu, D.; Zhao, X.-X.; Chen, Z.-T.; Ma, Y.-G. Synergistic Effect and Fluorination Effect in Ethylene Polymerization by Nickel Phenoxyiminato Catalysts. *Chin. J. Polym. Sci.* **2018**, *36*, 244–251.
- (16) Wang, J.; Yao, E.; Chen, Z.; Ma, Y. Fluorinated Nickel(II) Phenoxyiminato Catalysts: Exploring the Role of Fluorine Atoms in Controlling Polyethylene Productivities and Microstructures. *Macromolecules* **2015**, *48*, 5504–5510.
- (17) Saito, J.; Mitani, M.; Mohri, J.-i.; Yoshida, Y.; Matsui, S.; Ishii, S.-i.; Kojoh, S.-i.; Kashiwa, N.; Fujita, T. Living Polymerization of Ethylene with a Titanium Complex Containing Two Phenoxy-Imine Chelate Ligands. *Angew. Chem., Int. Ed.* **2001**, *40*, 2918–2920.
- (18) Saito, J.; Mitani, M.; Onda, M.; Mohri, J.-i.; Ishii, S.-i.; Yoshida, Y.; Nakano, T.; Tanaka, H.; Matsugi, T.; Kojoh, S.-i.; Kashiwa, N.; Fujita, T. Microstructure of Highly Syndiotactic “Living” Poly(propylene)s Produced from a Titanium Complex with Chelating Fluorine-Containing Phenoxyimine Ligands (an FI Catalyst). *Macromol. Rapid Commun.* **2001**, *22*, 1072–1075.
- (19) Mitani, M.; Mohri, J.-i.; Yoshida, Y.; Saito, J.; Ishii, S.; Tsuru, K.; Matsui, S.; Furuyama, R.; Nakano, T.; Tanaka, H.; Kojoh, S.-i.; Matsugi, T.; Kashiwa, N.; Fujita, T. Living Polymerization of Ethylene Catalyzed by Titanium Complexes Having Fluorine-Containing Phenoxy-Imine Chelate Ligands. *J. Am. Chem. Soc.* **2002**, *124*, 3327–3336.
- (20) Mitani, M.; Furuyama, R.; Mohri, J.-i.; Saito, J.; Ishii, S.; Terao, H.; Nakano, T.; Tanaka, H.; Fujita, T. Syndiospecific Living Propylene Polymerization Catalyzed by Titanium Complexes Having Fluorine-Containing Phenoxy-Imine Chelate Ligands. *J. Am. Chem. Soc.* **2003**, *125*, 4293–4305.
- (21) Matsui, S.; Tohi, Y.; Mitani, M.; Saito, J.; Makio, H.; Tanaka, H.; Nitabaru, M.; Nakano, T.; Fujita, T. New Bis(salicylaldiminato) Titanium Complexes for Ethylene Polymerization. *Chem. Lett.* **1999**, *28*, 1065–1066.
- (22) Tian, J.; Coates, G. W. Development of a Diversity-Based Approach for the Discovery of Stereoselective Polymerization Catalysts: Identification of a Catalyst for the Synthesis of Syndiotactic Polypropylene. *Angew. Chem., Int. Ed.* **2000**, *39*, 3626–3629.
- (23) Tian, J.; Hustad, P. D.; Coates, G. W. A New Catalyst for Highly Syndiospecific Living Olefin Polymerization: Homopolymers and Block Copolymers from Ethylene and Propylene. *J. Am. Chem. Soc.* **2001**, *123*, 5134–5135.
- (24) Hustad, P. D.; Coates, G. W. Insertion/Isomerization Polymerization of 1,5-Hexadiene: Synthesis of Functional Propylene Copolymers and Block Copolymers. *J. Am. Chem. Soc.* **2002**, *124*, 11578–11579.
- (25) Hustad, P. D.; Tian, J.; Coates, G. W. Mechanism of Propylene Insertion Using Bis(phenoxyimine)-Based Titanium Catalysts: An Unusual Secondary Insertion of Propylene in a Group IV Catalyst System. *J. Am. Chem. Soc.* **2002**, *124*, 3614–3621.
- (26) Mason, A. F.; Coates, G. W. New Phenoxyketimine Titanium Complexes: Combining Isotacticity and Living Behavior in Propylene Polymerization. *J. Am. Chem. Soc.* **2004**, *126*, 16326–16327.
- (27) Edson, J. B.; Wang, Z.; Kramer, E. J.; Coates, G. W. Fluorinated Bis(phenoxyketimine)titanium Complexes for the Living, Isolelective Polymerization of Propylene: Multiblock Isotactic Polypropylene Copolymers via Sequential Monomer Addition. *J. Am. Chem. Soc.* **2008**, *130*, 4968–4977.
- (28) Lamberti, M.; Pappalardo, D.; Zambelli, A.; Pellecchia, C. Syndiospecific Polymerization of Propene Promoted by Bis(salicylaldiminato)titanium Catalysts: Regiochemistry of Monomer Insertion and Polymerization Mechanism. *Macromolecules* **2002**, *35*, 658–663.
- (29) Milano, G.; Cavallo, L.; Guerra, G. Site Chirality as a Messenger in Chain-End Stereocontrolled Propene Polymerization. *J. Am. Chem. Soc.* **2002**, *124*, 13368–13369.
- (30) Talarico, G.; Busico, V.; Cavallo, L. Origin of the Regiochemistry of Propene Insertion at Octahedral Column 4 Polymerization Catalysts: Design or Serendipity? *J. Am. Chem. Soc.* **2003**, *125*, 7172–7173.
- (31) Prasad, A. V.; Makio, H.; Saito, J.; Onda, M.; Fujita, T. Highly Isospecific Polymerization of Propylene with Bis(phenoxy-imine) Zr and Hf Complexes Using $i\text{Bu}_3\text{Al}/\text{Ph}_3\text{CB}(\text{C}_6\text{F}_5)_4$ as a Cocatalyst. *Chem. Lett.* **2004**, *33*, 250–251.
- (32) Ishii, S.-i.; Furuyama, R.; Matsukawa, N.; Saito, J.; Mitani, M.; Tanaka, H.; Fujita, T. Ethylene and Ethylene/Propylene Polymerization Behavior of Bis(phenoxy-imine) Zr and Hf Complexes with Perfluorophenyl Substituents. *Macromol. Rapid Commun.* **2003**, *24*, 452–456.
- (33) Saito, J.; Onda, M.; Matsui, S.; Mitani, M.; Furuyama, R.; Tanaka, H.; Fujita, T. Propylene Polymerization with Bis(phenoxy-imine) Group-4 Catalysts Using $i\text{Bu}_3\text{Al}/\text{Ph}_3\text{CB}(\text{C}_6\text{F}_5)_4$ as a Cocatalyst. *Macromol. Rapid Commun.* **2002**, *23*, 1118–1123.
- (34) Lamberti, M.; Consolmagno, M.; Mazzeo, M.; Pellecchia, C. A Binaphthyl-Bridged Salen Zirconium Catalyst Affording Atactic Poly(propylene) and Isotactic Poly(α -olefins). *Macromol. Rapid Commun.* **2005**, *26*, 1866–1871.
- (35) Cuomo, C.; Strianese, M.; Cuenca, T.; Sanz, M.; Grassi, A. Olefin Polymerization Promoted by a Stereorigid Bridged Diiminobis-(phenolate) Zirconium Complex. *Macromolecules* **2004**, *37*, 7469–7476.
- (36) Camacho, D. H.; Salo, E. V.; Ziller, J. W.; Guan, Z. Cyclophane-Based Highly Active Late-Transition-Metal Catalysts for Ethylene Polymerization. *Angew. Chem., Int. Ed.* **2004**, *43*, 1821–1825.
- (37) Camacho, D. H.; Guan, Z. Living Polymerization of α -Olefins at Elevated Temperatures Catalyzed by a Highly Active and Robust Cyclophane-Based Nickel Catalyst. *Macromolecules* **2005**, *38*, 2544–2546.
- (38) Takano, S.; Takeuchi, D.; Osakada, K.; Akamatsu, N.; Shishido, A. Dipalladium Catalyst for Olefin Polymerization: Introduction of Acrylate Units into the Main Chain of Branched Polyethylene. *Angew. Chem., Int. Ed.* **2014**, *53*, 9246–9250.
- (39) Takeuchi, D.; Chiba, Y.; Takano, S.; Osakada, K. Double-Decker-Type Dinuclear Nickel Catalyst for Olefin Polymerization: Efficient Incorporation of Functional Co-monomers. *Angew. Chem., Int. Ed.* **2013**, *52*, 12536–12540.
- (40) Chen, Z.; Zhao, X.; Gong, X.; Xu, D.; Ma, Y. Macrocyclic Trinuclear Nickel Phenoxyimine Catalysts for High-Temperature Polymerization of Ethylene and Isospecific Polymerization of Propylene. *Macromolecules* **2017**, *50*, 6561–6568.
- (41) Yao, E.; Wang, J.; Chen, Z.; Ma, Y. Homo- and Heteroligated Salicylaldiminato Titanium Complexes with Different Substituents Ortho to the Phenoxy Oxygens for Ethylene and Ethylene/1-Hexene (Co)polymerization. *Macromolecules* **2014**, *47*, 8164–8170.
- (42) Falivene, L.; Credendino, R.; Poater, A.; Petta, A.; Serra, L.; Oliva, R.; Scarano, V.; Cavallo, L. SambVca 2. A Web Tool for Analyzing Catalytic Pockets with Topographic Steric Maps. *Organometallics* **2016**, *35*, 2286–2293 and references therein. See also <https://www.molnac.unisa.it/OMtools/sambvca2282.2280/index.html>.
- (43) Resconi, L.; Waymouth, R. M. Diastereoselectivity in the Homogeneous Cyclopolymerization of 1,5-Hexadiene. *J. Am. Chem. Soc.* **1990**, *112*, 4953–4954.
- (44) Salata, M. R.; Marks, T. J. Catalyst Nuclearity Effects in Olefin Polymerization. Enhanced Activity and Comonomer Enchainment in Ethylene + Olefin Copolymerizations Mediated by Bimetallic Group 4 Phenoxyiminato Catalysts. *Macromolecules* **2009**, *42*, 1920–1933.
- (45) Mazzeo, M.; Strianese, M.; Lamberti, M.; Santoriello, L.; Pellecchia, C. Phenoxyaldimine and Phenoxyketimine Titanium Complexes in Propene Polymerization. A Different Effect of *o*-Phenoxy Halide Substituents. *Macromolecules* **2006**, *39*, 7812–7820.
- (46) Lindeman, L. P.; Adama, J. Q. Carbon-13 Nuclear Magnetic Resonance Spectrometry. Chemical Shifts for the Paraffins through C_9 . *Anal. Chem.* **1971**, *43*, 1245–1252.